Anal Bioanal Chem
DOI 10.1007/s00216-017-0657-3

RESEARCH PAPER

# Isolation and identification of human metabolites from a novel anti-tumor candidate drug 5-chlorogenic acid injection by HPLC-HRMS/MS$^n$ and HPLC-SPE-NMR

**Tiankun Ren[1] · Yanan Wang[1] · Caihong Wang[1] · Mengtian Zhang[2] · Wang Huang[2] · Jiandong Jiang[1] · Wenbin Li[3] · Jinlan Zhang[1]**

Received: 10 June 2017 / Revised: 4 September 2017 / Accepted: 19 September 2017


**Abstract** A novel anti-tumor candidate drug, 5-chlorogenic acid (5-CQA) injection, was used for the treatment of malignant glioma in clinical trial (phase I) in China. The isolation and identification of the metabolites of 5-CQA injection in humans were investigated in the present study. Urine and feces samples obtained after intramuscular administration of 5-CQA injection to healthy adults have been analyzed by high-performance liquid chromatography coupled with high-resolution mass and multiple-stage mass spectrometry (HPLC-HRMS/MS$^n$). No metabolite was detected in human feces; however, in human urine, a total of six metabolites were identified including isomerized 5-CQA (P1 and P2), hydrolyzed 5-CQA (M1and M2), and methylated 5-CQA (M3 and M4). Among them, M3 and M4 were the main metabolites and target analytes for human mass balance study. Additionally, the structure of M3 and M4 was characterized by high-performance liquid chromatography-solid phase extraction-nuclear magnetic resonance (HPLC-SPE-NMR), and the results demonstrated that the methoxy group of M3 and M4 was exclusively attributed to C-3′ and C-4′, respectively. Due to the unavailability of commercial reference, the pure products of M3 and M4 were synthesized by 5-CQA methylation and followed by isolation and purification. Moreover, the potential activity of M3 and M4 on malignant glioma was predicted using a reverse molecular docking analysis on eight malignant glioma-related pathways. The results showed that M3 and M4 had various interactions against malignant glioma-related targets. Our study provides an insight into the metabolism of 5-CQA injection in humans and supports the clinical human mass balance study.

**Keywords** Human urine · Metabolites · 5-Chlorogenic acid (5-CQA) · Identification · High-performance liquid chromatography coupled with high-resolution mass and multiple-stage mass spectrometry (HPLC-HRMS/MS$^n$) · High-performance liquid chromatography-solid phase extraction-nuclear magnetic resonance (HPLC-SPE-NMR)

Tiankun Ren and Yanan Wang contributed equally to this work.

**Electronic supplementary material** The online version of this article (https://doi.org/10.1007/s00216-017-0657-3) contains supplementary material, which is available to authorized users.

✉ Jiandong Jiang
jiangjd@imm.ac.cn

✉ Wenbin Li
liwenbin@ccmu.edu.cn

✉ Jinlan Zhang
zhjl@imm.ac.cn

[1] State Key Laboratory of Bioactive Substance and Function of Natural Medicines, Institute of Materia Medica, Peking Union Medical College & Chinese Academy of Medical Sciences, No. 2 Nanwei Street, Xicheng District, Beijing 100050, China

[2] Jiuzhang Biochemical Engineering Science and Technology Development Co., Ltd., Chengdu, Sichuan 610041, China

[3] Department of Glioma, Beijing Shijitan Hospital, Capital Medical University, Beijing 100038, China

**Abbreviations**

| | |
|---|---|
| CQA | Chlorogenic acid |
| HMBC | Heteronuclear multiple bond correlation |
| HPLC-HRMS/MS$^n$ | High-resolution mass and multiple-stage mass spectrometry |

Published online: 07 November 2017

| | |
|---|---|
| HPLC-SPE-NMR | High-performance liquid chromatography-solid phase extraction-nuclear magnetic resonance |
| HSQC | Heteronuclear single-quantum correlation |

## Introduction

Chlorogenic acids (CQAs) are a family of esters formed by trans-cinnamic acids and D-(-)-quinic acid [1], which serve as the bioactive compounds of herbal medicines such as the flower of *Lonicera japonica* Thunb and the leaves of *Eucommia ulmoides* [2]. The most widely occurring CQA in plants and medicinal herbs is 5-O-caffeoylquinic acid [(1S,3R,4R,5R)-3-{[(2Z)-3-(3,4-dihydroxyphenyl) prop-2-enoyl]oxy}-1,4,5-trihydroxycyclohexanecarboxylic acid; 5-CQA] [3]. Accumulating evidence has demonstrated that CQAs exhibited multiple pharmacological properties, including antibacterial, antioxidant, analgesic, antipyretic, and anticarcinogenic activities [4–7]. Moreover, 5-CQA has been proposed to inhibit tumor growth and angiogenesis by suppressing tyrosinase and matrix metalloproteinase (MMP)-9 [8, 9] or by inhibiting HIF-1α stabilization and AKT phosphorylation [10]. The 5-CQA injection is a novel anti-tumor candidate drug developed by Sichuan J.Z. Bio-chemical Science and Technology Development Co., Ltd., in China. The clinical approval documents of the raw materials and injection of 5-CQA (approval number 2013L01856 and 2013L1855) were promulgated by CFDA in 2013. Currently, the phase I clinical trial of tolerance and pharmacokinetics characters of 5-CQA injection in the advanced malignant tumor subjects is being carried out at Beijing Shijitan Hospital in China.

Metabolites play an important role in clinical research since they are closely related to the clinic efficacy and toxicity. For example, lovastatin had no activity in vitro; however, it could be hydrolyzed to β-hydroxy acid derivatives in vivo to form an effective inhibitor for HMG-CoA reductase which contributed to the treatment of coronary heart disease [11]. Some drugs were easy to be metabolic inactivation in the body at the end of treatment, because they were decomposed and rapidly excreted out of the body according to the pre-set metabolic pathway, thereby avoiding the toxicity. Atracurium besilate, a kind of muscle relaxant, was quickly metabolized to inactive metabolites under physiological conditions. There was no accumulation of atracurium besilate in the body, which had no harm to the heart, liver, and kidney [12]. Other drugs like lidocaine produced toxic metabolites. It was metabolized in the liver to form the ethyl metabolites which still had a local anesthesia effect and lead to a certain toxicity [13]. Therefore, metabolism could make the drugs produce active, inactive, and even toxic metabolites, so the analysis and identification of the drug metabolites are of great significance in clinical trials.

The absorption of orally administered 5-CQA and caffeic acid was previously studied in rats [14]. Rats were administered 248 mg/kg of 5-CQA or caffeic acid, and the blood was collected from the tail for 6 h after administration. After 5-CQA administration, only traces of caffeic and ferulic acid conjugates appeared in the plasma, and no 5-CQA was detected. However, 5-CQA and a variety of its metabolites were found in the plasma after caffeic acid administration. Therefore, it is speculated that 5-CQA is not easily absorbed by the intestine, but can be first hydrolyzed to caffeic acid and then be absorbed by the intestine. Urinary metabolites of caffeic acid and 5-CQA were studied by Booth et al. [15]. After oral administration of 1 g of 5-CQA to volunteers, the major metabolites in urine were caffeic acid, glycine conjugates of m-hydroxy coumaric acid, glucuronic acid conjugates, and dihydromuric acid. Thus, the main products of 5-CQA in plasma or urine were caffeic acid and its metabolites. Unlike oral administration, 5-CQA was extensively metabolized in rats after a single intravenous administration of 10 mg/kg [16], and a total of 35 metabolites were detected in the bile, urine, feces, and plasma. The major metabolites in bile were glutathione conjugates of methylated 5-CQA, occupying approximately 80% of the metabolites excreted in the bile. The predominant components in urine were 5-CQA, methylated 5-CQA, hydrolyzed metabolites, and glucuronide conjugates. The major metabolites in the feces were methylated 5-CQA and its cysteine conjugates. These results demonstrated that 5-CQA underwent wide metabolism in rats. It is remarkable that there are no reports of 5-CQA metabolism in humans after intramuscular administration so far.

In this paper, the metabolic profile of 5-CQA injection in human urine and feces were investigated by HPLC-HRMS/$MS^n$ after the intramuscular administration. The metabolites were identified based on HRMS and $MS^n$ data, and the principal methylated metabolites were unambiguously assigned based on NMR data by HPLC-SPE-NMR. Moreover, main metabolites in humans were synthetized for the support of human mass balance study. The activity of main metabolites on anti-malignant glioma was predicted by reverse molecular docking method.

## Materials and methods

### Chemicals and reagents

The 5-CQA raw materials (purity 99.6%) and 5-CQA injection (purity 99.7%, 120 mg per injection, containing 30 mg of 5-CQA) were supplied by Sichuan Jiuzhang Bio-Technique Co. Ltd. (Sichuan, China). Both purities were measured by the method of metabolite profile. Caffeic acid and 5-CQA

standards were purchased from the National Institute for Control of Pharmaceutical and Biological Products (Beijing, China). Quinic acid standard was obtained from Sigma-Aldrich (St. Louis, MO, USA). The purity of all standards was greater than 96%. Methanol of MS grade and HPLC grade was purchased from Fisher Chemicals Co. (Fair Lawn, NJ, USA) and Honeywell Burdick & Jackson Inc. (Muskegon, MI, USA). Trifluoroacetic acid of analytical grade was obtained from J&K Scientific Ltd. (Beijing, China). Formic acid of HPLC grade was purchased from Mallinckrodt Baker Inc. (Phillipsburg, NL, USA). Dimethyl sulfate of analytical grade was ordered from Shenyang Chemical Reagent Plant (Shenyang, China). Triethylamine of analytical grade was from Fisher Chemicals Co. (Fair Lawn, NJ, USA). Tetra-n-butylammonium bromide of analytical grade was obtained from Shanghai Dibai Chemical Technology Co. (Shanghai, China). Sodium hydroxide of analytical grade was purchased from Beijing Chemical Reagent Plant (Beijing, China). Other chemicals were all of analytical grade. Deionized water was purified using a Millipore water purification system (Millipore, Billerica, MA, USA).

## Human urine and feces collection

Three healthy adults were enrolled in this study, including a male adult and two female adults aged from 31 to 45 years with a mean body weight of 60 kg.

A single dose of 120 mg 5-CQA injection (corresponding to 30 mg of 5-CQA) was intramuscularly administered to three adults each day, and the administration lasted for five consecutive days. Blank urine and feces were collected before administration. Urine was taken in three fractions (0–3, 3–4, and 4–6 h) on the first day and 0–3 h from the second day to the fifth day after drug administration. Feces were collected 0–24 h on the first day after dosing. The obtained urine and feces were frozen at − 80 °C immediately for further use.

## Metabolic profile by HPLC-HRMS/MS$^n$

### *Sample preparation*

After thawing at 4 °C, a 1-mL of urine sample from each participant at different fractions on the first day was transferred into a 10-mL glass tube. An aliquot of 5 mL methanol was added to the tube, after which the mixture was sonicated for 5 min and centrifuged at 4500 rpm for 10 min. The supernatant was then collected and evaporated to dryness at 37 °C under a gentle stream of nitrogen. The residue was redissolved in 100 μL of water containing 1% formic acid-methanol (9:1, *v*/*v*) and centrifuged at 10000 rpm for 10 min. A 20-μL supernatant was injected into the HPLC-HRMS system for analysis.

Fecal samples were dried in the dark at room temperature and slowly ground into powder. Then a 0.2 g of fecal sample from each participant was extracted with 1 mL methanol by ultrasonic treatment for 10 min and subsequently centrifuged at 3500 rpm for 5 min. An aliquot of 100 μL supernatant was transferred to another tube and then added 200 μL acetonitrile, followed by vortexing for 60 s. After that, the sample was centrifuged at 4500 rpm for 5 min, and the supernatant was evaporated to dryness at 37 °C under a gentle stream of nitrogen. The residue was redissolved in 100 μL water containing 1% formic acid-methanol (9: 1, *v*/*v*), and centrifuged at 10000 rpm for 10 min. A 20-μL of supernatant was injected into the HPLC-HRMS system for analysis.

### *HPLC-HRMS/MS$^n$ analytical condition*

HPLC separation was carried out on a Surveyor LC Plus system equipped with a Surveyor MS Pump Plus, a Surveyor Autosampler, and a Surveyor PDA Plus detector. Samples were separated on a Waters Symmetry C18 column (250 mm × 4.6 mm, 3 μm). The mobile phase consisted of 0.1% formic acid in water (A) and methanol (B) delivered at a flow rate of 0.9 mL/min (split ratio, 1: 3) using a gradient program as follows: 0–3 min, 10% B; 15–16 min, 45% B; 21 min, 90% B; 24–30 min, 10% B. Column temperature was maintained at 30 °C. UV detection was set at 330 nm and the spectra were collected at 200–600 nm.

A Thermo Scientific LTQ FT was connected to the Thermo Scientific Surveyor LC Plus system by an electrospray ionization (ESI) interface. Ultrahigh-purity helium (He) and high-purity nitrogen ($N_2$) were used as the collision gas and the nebulizing gas, respectively. The operating parameters in the negative ion mode were set as follows: ion spray voltage at 3.8 kV, capillary temperature at 250 °C, capillary voltage at − 45 V, sheath gas flow rate of 40 (arbitrary units), auxiliary gas flow rate of 10 (arbitrary units), sweep gas flow rate of 3 (arbitrary units), and tube lens at − 120 V. During the detection, the period of 0–1 min was switched to waste. Compounds were detected by full-scan mass analysis from *m/z* 100 to 1000 at a resolving power of 50,000 with data-dependent $MS^2$ analysis triggered by the two most abundant ions from full-scan mass analysis, followed by $MS^3$ analysis of the most abundant product ions. Collision-induced dissociation (CID) was performed with an isolation width of 2 Da. The collision energy was set as 35%. Dynamic exclusion was conducted by utilizing a repeat count of one, prior to exclusion. Each mass-to-charge value resided on the dynamic exclusion list for 30 s after the data-dependent $MS^2$ experiment. Upon data-dependent analyses incorporating dynamic exclusion, HRMS and $MS^n$ data of compounds in samples could be acquired automatically.

## Identification of methylated metabolites

### *Sample preparation*

A 50-μL prepared urine sample was diluted to 250 μL with water, then vortexed for 30 s, and centrifuged at 10000 rpm for 10 min. The supernatant was injected to HPLC system for analysis.

A 10-mg sample of 5-CQA raw materials was accurately weighed, then transferred to a 15-mL tube with 1.7 mL water, and vortexed for 30 s. An 850-μL 0.3 mmol/L NaOH was added to the tube; after which, the tube was vortexed for 30 s. The phase transfer catalyst tetra-n-butylammonium bromide was then added and the sample was vortexed again for 30 s. After adding 170 μL dimethyl sulfate, the tube was incubated for 15 min at 37 °C. A 170-μL triethylamine was added to the mixture and vortexed for 30 s. The mixture was then filtered through a 0.45-μm Millipore filter. An aliquot of 20 μL of filtered sample was diluted to 800 μL with water, then vortexed for 30 s, and centrifuged at 10000 rpm for 10 min. The supernatant was injected to HPLC system for analysis.

A 50-μL prepared urine sample and a 50-μL prepared synthetic sample were mixed to form the pooled sample and then vortexed for 30 s for HPLC analysis.

### *Comparison of methylated metabolites from human urine with chemical synthesis*

Two kinds of modes (mode A and mode B) were established to compare the methylated metabolites from human urine with chemical synthesis.

Both modes were carried out on a Surveyor LC Plus system equipped with a Surveyor MS Pump Plus, a Surveyor Autosampler, and a Surveyor PDA Plus detector. Samples were separated on a Waters Symmetry C18 column (250 mm × 4.6 mm, 3 μm). Column temperature was maintained at 30 °C, and the injection volume was 20 μL. UV detection was set at 330 nm and the spectra were collected at 200–600 nm.

The mobile phase of the mode A consisted of a mixture of 0.1% formic acid in water and methanol (75: 25, *v*/*v*). Analytes were eluted from the column over a 30-min run-time at a flow rate of 0.9 mL/min (split ratio, 1: 3). A Thermo Scientific LTQ FT was connected to the Thermo Scientific Surveyor LC Plus system by an electrospray ionization (ESI) interface. The HRMS condition was the same as metabolic profile.

The mode B was set as follows. The mobile phase consisted of 0.1% trifluoroacetic acid in water (A) and methanol (B) using a gradient program: 0–26 min, 26% B; 26.10–30 min, 80% B; 30.10–38 min, 26% B. The flow rate was set as follows: 0–26.10 min, 0.8 mL/min; 26.10–30 min, 0.8–1.2 mL/min; 30.10–38 min, 0.8 mL/min.

## HPLC-SPE-NMR analytical condition

The HPLC separation was performed with an Agilent 1260 system consisting of a degasser, a quaternary pump, an autosampler, a column oven, a diode array detector, and a Waters symmetry C18 column (250 mm × 4.6 mm, 3 μm). The column was operated at 30 °C. Separations were performed using the mode B. The HPLC eluate was directed to the photodiode-array detector and then, after diluting with 3 mL/min of $H_2O$ by means of a Knauer Smartline pump 120 (Knauer, Berlin, Germany), to a Prospect 2 SPE-unit (Spark Holland, Emmen, The Netherlands). Selected target chromatographic peaks were trapped on SPE cartridges (Hysphere GP-phase, 10 × 2 mm i.d., from Spark Holland), preconditioned with 6000 μL of MeOH and subsequently equilibrated with 500 μL of $H_2O$. A total of 20 cumulative trappings were performed for peaks M3 and M4 after 20 repeated separations using injections corresponding to synthetic sample. After trapping, the cartridges were dried with a stream of nitrogen gas for 30 min and subsequently eluted with methanol-$d_4$ into 3 mm o.d. NMR tubes (NORELL, Morganton, USA). The tubes were filled with 120 μL of eluted sample and sealed with plastic balls. Chromatographic separation and analyte trapping on SPE cartridges were controlled using the Hystar ver. 3.2 software (Bruker Daltonik).

NMR experiments were performed with a Bruker Avance III HD NMR system (operating at a $^1$H frequency of 600.25 MHz) equipped with a Bruker SampleXpress sample changer and a cryogenically cooled gradient observe 5 mm CPDCH probe head (Bruker Biospin, Karlsruhe, Germany) optimized for $^1$H and $^{13}$C observation. Bruker standard pulse sequences were used throughout this study. The 1D $^1$H NMR spectra were acquired in automation (temperature equilibration to 298 K, optimization of lock parameters, gradient shimming, and setting of receiver gain) with 30-degree pulses. A total of 65 k data points were collected and multiplied with an exponential function corresponding to line broadening of 0.3 Hz prior to Fourier transform. The 2D heteronuclear experiments were acquired with 1024 data points in the direct dimension and 220 data points in the indirect dimension (HSQC) or 4096 data points in the direct dimension and 300 data points in the indirect dimension (HMBC). The HMBC and HSQC experiments were optimized for $^nJ_{H,C}$ = 8 Hz and $^1J_{H,C}$ = 145 Hz, respectively. HMBC and HSQC spectra were processed to 1 k × 1 k data matrices, after linear prediction (32 coefficients) in F1 and application of a sine-bell window function in F1 and F2.

### Synthesis, isolation, and purification of methylated metabolites

*Synthesis*

A total of 200 mg 5-CQA raw materials were used for the synthesis and aliquoted into 20 copies. For each copy, 10 mg of 5-CQA raw materials, accurately weighed, was transferred to a 15-mL tube with 1.7 mL water and vortexed for 30 s. After addition of 850 μL of 0.3 mmol/L NaOH, the mixture was vortexed for 30 s again. The phase transfer catalyst tetra-n-butylammonium bromide was then added, and the sample was vortexed again for 30 s. After adding 170 μL of dimethyl sulfate, the tube was incubating 15 min at 37 °C. A 170-μL triethylamine was added into the mixture and vortexed for 30 s. An 8.7-mL diethyl ether was added into the mixture, followed by high-speed vortexing for 3 min.

Meanwhile, 20 μL of sample before and after diethyl ether extraction was diluted with 180 μL water, respectively, then vortexed for 30 s, and centrifuged at 10000 rpm for 10 min. The supernatant was injected to HPLC system for analysis.

Then 20 samples were centrifuged at 4500 rpm for 10 min. The lower aqueous phases were collected and transferred to a new tube for freeze-drying. At the same time, 20 μL of aqueous phase sample was diluted to 200 μL with water, then vortexed for 30 s, and centrifuged at 10000 rpm for 10 min. The supernatant was injected to HPLC system for analysis.

*HPLC-UV analytical condition*

Separation was carried out on a Surveyor LC Plus system equipped with a Surveyor MS Pump Plus, a Surveyor Autosampler, and a Surveyor PDA Plus detector. Samples were separated on a Waters Symmetry C18 column (250 mm × 4.6 mm, 3 μm). The mobile phase consisted of 0.1% formic acid in water (A) and methanol (B) using an isocratic elution program of 25% B for 30 min. The flow rate was set at 0.9 mL/min (split ratio, 1: 3). Column temperature was maintained at 30 °C. UV detection was set at 330 nm and the spectra were collected at 200–600 nm.

*Isolation and purification*

After freeze-drying, the synthesized sample was dissolved in 3 mL water containing 0.01% formic acid and then centrifuged at 4500 rpm for 10 min. The supernatant was subjected to an ODS column (200–300 mesh, 60 g) using a step-wise system of methanol/$H_2O$ contain 0.01% formic acid (0:100, 10:90, 20:80, 30:70, 40:50, 60:40, 100:0, *v*/*v*, each 200 mL) under gradient elution to yield seven fractions (A–G). Fractions A–G were analyzed by an established HPLC method (the HPLC method was the same as HPLC-UV analytical condition), and the results showed that M3 and M4 were enriched in fraction E.

Semipreparative HPLC for the isolation of M3 and M4 was performed on Shimadzu LC-6AD system (Shimadzu, Kyoto, Japan). After freeze-drying, the fraction E was dissolved in 1.5 mL water and vortexed for 30 s. The sample was centrifuged at 13000 rpm for 10 min. The supernatant was loaded on semipreparative HPLC using an Agilent XDB-C18 (9.4 × 250 mm, 5 μm). The mobile phases consisted of 0.1% formic acid in water (A) and methanol (B). The isocratic elution used 25% B for 40 min at a flow rate of 5 mL/min. The detection wavelength was set at 330 nm. The eluents of M3 and M4 were collected and evaporated to appropriate volume for freeze-drying, respectively.

### Data analysis

MS data acquisition was performed with the Xcalibur version 2.0 SR2 software (Thermo Fisher Scientific, San Jose, CA, USA). The identification of metabolites was carried out with the Metwork 1.3 software (Thermo Fisher Scientific, San Jose, CA, USA).

Topspin ver. 3.2 patch level 7 (Bruker Biospin) was used for acquisition and processing of NMR data, whereas IconNMR ver.4.7.7 (Bruker Biospin) was used for controlling automated sample change and acquisition.

To determine whether the compounds were associated with malignant glioma, reverse molecular docking was performed to predict the activities of methylated metabolites as well as 5-CQA. The method was based on the previous study of our laboratory [17]. Briefly, PharmMapper (http://lilab.ecust.edu.cn/pharmmapper/) was used to carry out a reverse molecular analysis for the discovery of potential targets. Next, the predicted targets were labeled in eight malignant glioma-related pathways using KEGG (http://www.kegg.jp/). These typical pathways include the PI3K-Akt, mTOR, Ras, EGFR, MAPK, NF-kappa B, and Jak-STAT pathways and DNA replication [18–22].

## Results

### Metabolic profile of dosed human urine and feces by HPLC-HRMS/$MS^n$

The HPLC-HRMS/$MS^n$ method was established for metabolic profile of human biosamples based on the previous analytical method [16]. Some modification was performed including the change to a longer size column (from Phenomenex Luna C18 (150 mm × 4.6 mm, 5 μm) to Waters Symmetry C18 column (250 mm × 4.6 mm, 3 μm)) and the optimization of the gradient elution program to get efficient separation of 5-

CQA and its metabolites in biological samples. The optimized chromatograms of human urine and feces are shown in Fig. 1.

For the MS condition, the ionization polarity was optimized by comparing the mass response of 5-CQA, M3, and M4 in human urine samples. As shown in the Electronic Supplementary Material (ESM, Fig. S1), the negative ion mode was chosen. The MS data acquisition mode was data-dependent scanning coupled with the dynamic exclusion technique to collect $MS^n$ data automatically. The $MS^{n+1}$ data-dependent scanning was performed on the basis of the two most abundant ions of $MS^n$ scan mass data. The dynamic exclusion technique was used to collect the $MS^n$ data promptly, which sets up a dynamic depot to exclude all collected parent ions. After optimization, primary setting parameters for the dynamic exclusion were set as follows: repeat count, 1; repeat duration, 10 s; exclusion list size, 50; and exclusion duration, 30 s.

For the preparation of urine samples, preparation methods (lyophilization and precipitation) and redissolved solutions (methanol and initial mobile phase) were optimized. The results indicated that lyophilization was not effective to the extraction of methylated metabolites (ESM, Fig. S2) compared with methanol precipitation. Besides, the initial mobile phase was more beneficial to the recovery of 5-CQA and methylated metabolites (ESM, Fig. S2). So, methanol precipitation and redissolution with the initial mobile phase were chosen as the preparation method. For the preparation of fecal samples, two different redissolved solutions (methanol and initial mobile phase) were compared. The results showed that no metabolite was detected in the feces, no matter which solvent is used.

As shown in Fig. 1a–c, the concentration of 5-CQA is too high in 0–3 h urine sample. To avoid unexpected residual contamination to MS instrument, the 5-CQA peaks (Rt 13.5–14.5 min) in this sample was switched to waste. Others samples were analyzed without the action, due to the safe concentration of 5-CQA. The metabolic profiles of blank urine and feces before 5-CQA administration were shown in ESM (Fig. S15). As shown in ESM Fig. S15, an obvious endogenous compound peak with retention time at 19.6 min appeared in the HPLC-UV chromatogram of blank urine. As for blank feces, there was no obvious peak appeared in the HPLC-UV chromatograms.

The metabolites were identified based on HRMS and $MS^n$ data. It can be found that a total of six metabolites, along with 5-CQA, were identified in human urine (Fig. 1), whereas no metabolite was detected in human feces by HPLC-LTQ/FTICR-MS. As shown in Fig. 1, the most abundant drug-related component was 5-CQA. The major metabolites in the urine were M3 and M4, which were eluted at 16.53 and 17.16 min, respectively. After comparing with the

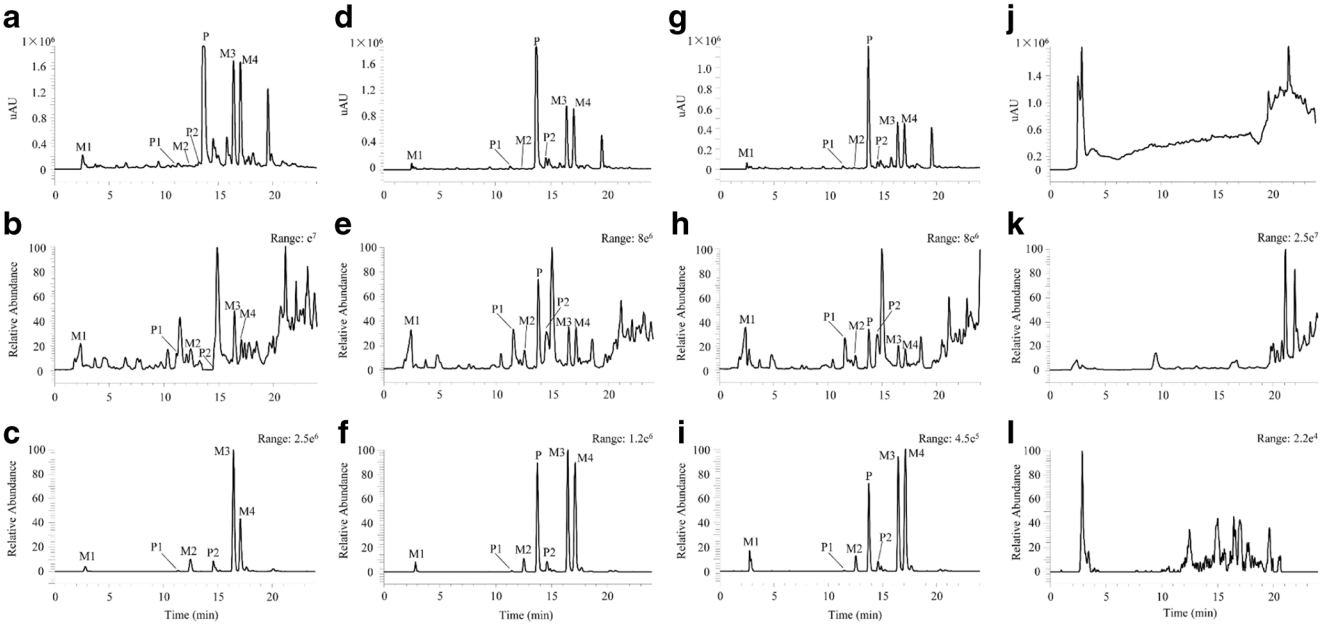


**Fig. 1** Metabolic profiles of 5-CQA after a single intramuscular administration of 120 mg of 5-CQA injection to humans. **a** HPLC-UV chromatogram of metabolites detected in human urine during 0–3 h. **b** Total ion chromatogram of metabolites detected in human urine during 0–3 h. **c** Extracted ion current chromatogram of metabolites detected in human urine during 0–3 h. **d** HPLC-UV chromatogram of metabolites detected in human urine during 3–4 h. **e** Total ion chromatogram of metabolites detected in human urine during 3–4 h. **f** Extracted ion current chromatogram of metabolites detected in human urine during 3–4 h. **g** HPLC-UV chromatogram of metabolites detected in human urine during 4–6 h. **h** Total ion chromatogram of metabolites detected in human urine during 4–6 h. **i** Extracted ion current chromatogram of metabolites detected in human urine during 4–6 h. **j** HPLC-UV chromatogram of metabolites detected in human feces during 0–24 h. **k** Total ion chromatogram of metabolites detected in human feces during 0–24 h. **l** Extracted ion current chromatogram of metabolites detected in human feces during 0–24 h

chromatogram of blank urine before 5-CQA injection, we found out the relatively large peak eluted after M4 was an obvious endogenous compound from blank human urine matrix as shown in Fig. 1a, d, e. It was not a metabolite of 5-CQA. Table 1 lists detailed information about the metabolites detected in human urine, including the proposed structures, protonated molecular ions, retention times, and characteristic fragment ions. The metabolites were named in the serial order of their retention times.

**Parent drug P** A chromatographic peak was detected at 13.79 min in human urine. It gave a protonated molecular ion

**Table 1** Identification of metabolites in human urine after an intramuscular administration of 120 mg of 5-CQA injection using HPLC-LTQ/FTICR-MS

| No. | Proposed Structure | RT (time) | $[M-H]^-$ | Proposed Formula | Error (ppm) | Fragment Ions |
|---|---|---|---|---|---|---|
| M1 | 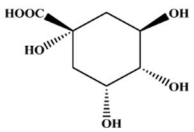 | 2.94 | 191.0560 | $C_7H_{11}O_6$ | -0.56 | $MS^2$[191]:173(100) |
| P1 | 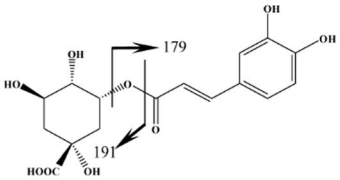 | 11.45 | 353.0876 | $C_{16}H_{17}O_9$ | -0.58 | $MS^2$[353]:191(100),179(33); $MS^3$[191]:85(100) |
| M2 | 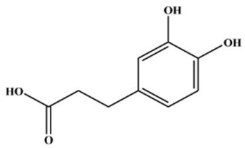 | 12.57 | 181.0505 | $C_9H_9O_4$ | -0.73 | $MS^2$[181]:121(100) |
| P | 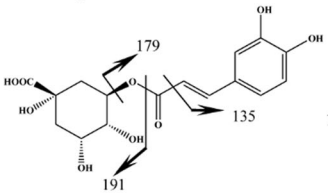 | 13.79 | 353.0879 | $C_{16}H_{17}O_9$ | 0.27 | $MS^2$[353]:191(100), 179(4), 135(1); $MS^3$[191]:85(100) |
| P2 | 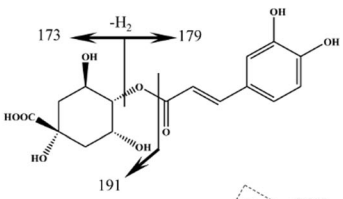 | 14.63 | 353.0878 | $C_{16}H_{17}O_9$ | -0.02 | [353]:173(100),179(56),191(44); [173]:93(100) |
| M3 | 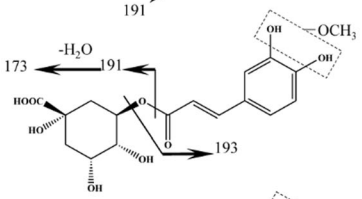 | 16.53 | 367.1031 | $C_{17}H_{19}O_9$ | -0.97 | [367]:191(100),193(6); [191]:127(100),173(62) |
| M4 | 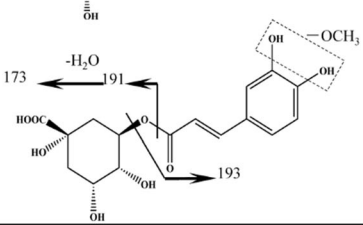 | 17.16 | 367.1035 | $C_{17}H_{19}O_9$ | 0.12 | [367]:173(100), 193(5),191(1); [173]:93(100) |

at *m/z* 353.0879, indicating that its elemental composition was $C_{16}H_{17}O_9$ with an error of − 0.56 ppm. The main characteristic product ions of *m/z* 353.0879 were observed at *m/z* 191, 179, 135, and 85. The fragment ions at *m/z* 191 ([quinic acid-H]$^-$) and 179 ([caffeic acid-H]$^-$) were formed by the hydrolysis of the ester bond. The fragment ion at *m/z* 135 was formed via the loss of $CO_2$ from the fragment ion at *m/z* 179, while *m/z* 85 was proposed to form via the cleavage of the C–C bond and the loss of $CO_2$ from the fragment ion at *m/z* 191. The retention time was identical to the standard of 5-CQA, indicating that this component was unmetabolized 5-CQA, designated as the parent drug (P). The P was the most abundant component in human urine and was not found in human feces.

**P1 and P2** Metabolites P1 and P2 were found in human urine. With the chemical formula of $C_{16}H_{17}O_9$, they displayed [M-H]$^-$ ion at *m/z* 353.0876 and 353.0878, respectively. P1 and P2 had the same elemental composition with parent drug, illustrating they were isomers of 5-CQA. P1 and P2 showed the base peak at *m/z* 191 and *m/z* 173, respectively. According to the previous study [16], isomers can be distinguished by their chromatographic and characteristic MS fragmentation behaviors. Briefly, neochlorogenic acid showed the base peak at *m/z* 191.053; however, a strong key ion was observed at *m/z* 179.034 ([caffeic acid-H]$^-$) formed by the cleavage of the alkyl C–O bond adjacent to the ester. Cryptochlorogenic acid exhibited the base peak ion at *m/z* 173.044 ([quinic acid-$H_2O$-H]$^-$), which was a characteristic ion for the isomer with caffeic acid substituted at position 4 and formed by the cleavage of the alkyl C–O bond adjacent to the ester. Therefore, P1 and P2 were demonstrated as neochlorogenic acid and cryptochlorogenic acid, respectively.

**M1** Metabolite M1, found in urine, was eluted at 2.94 min. Its protonated molecular weight was 191.0560 and was the same as [quinic acid-H]$^-$. The elemental composition of M1 was $C_7H_{11}O_6$. M1 formed fragment ion at *m/z* 173 by losing of 18 Da, suggesting the loss of a $H_2O$. The retention time of M1 was the same as the standard of quinic acid. Therefore, metabolite M1 was identified as the hydrolyzed metabolite of the parent drug named quinic acid.

**M2** Metabolite M2, detected in urine with a retention time of 12.57 min, exhibited a [M-H]$^-$ peak at *m/z* 181.0505 corresponding to $C_9H_9O_4$, which indicated the loss of $C_7H_8O_5$ from 5-CQA. M2 was 2 Da higher than the fragment ion at *m/z* 179 ([caffeic acid-H]$^-$) which was the hydrolyzed product of the parent drug. High-collision energy analysis revealed product ions of M2 at *m/z* 121, indicating that rearrangement of carboxyl was occurred. So M2 was accordingly confirmed as the reduced metabolite of the caffeic acid.

**M3 and M4** Metabolite M3 and M4 were eluted at 16.53 and 17.16 min, respectively, with [M-H]$^-$ ion at *m/z* 367.1031 and 367.1035 in ESI (-). The elemental composition of M3 and M4 was $C_{17}H_{19}O_9$, indicating the methylation 5-CQA. Both M3 and M4 formed fragment ion at *m/z* 193 by adding of 14 Da comparing with [caffeic acid-H]$^-$, suggesting that a $CH_2$ was attached to one of the phenolic hydroxyl groups on the benzene ring. The exact methylation site of M3 and M4 needs further data to confirm.

## Identification of methylated metabolites by HPLC-NMR

As shown in Fig. 2, the retention times of M3 and M4 in the synthetic sample were equal to those in the urine sample as well as the pooled sample comparing by two kinds of modes. The methylated products M3 and M4 from chemical synthesis and human urine were identified as the same compounds according to the EU Directive 2002-657-EC (http://eur-lex.europa.eu/eli/dec/2002/657/oj) (ESM, Figs. S3–S4) by the HRMS and $MS^n$ data (ESM, Table S3). It was reliable to use synthetic samples instead of human urine samples for the identification of M3 and M4.

As shown in ESM (Fig. S16), the $^1$H NMR spectrum of the content of peak 1 ($t_R$ = 18.65–20.07 min, M3) obtained in the HPLC-SPE-NMR mode showed an additional set of resonances ($\delta_H$ 3.84 for M3) for a methoxyl, compared with 5-CQA. This was consistent with our previous observation during comparison of HRMS spectra of M3 and 5-CQA. It was therefore decided to perform a more thorough HPLC-SPE-NMR analysis, including acquisition of 2D heteronuclear (HSQC and HMBC) experiments as shown in the Electronic Supplementary Material (ESM, Figs. S5–S8). The spectrum data of M3 listed in Table 2 revealed signals for one caffeic acid moiety and one quinic acid moiety. The position of the methoxyl group was confirmed by coupling between the methoxy protons ($\delta_H$ 3.84) and C-3′ ($\delta_C$ 149.4) as well as between H-2′ ($\delta_H$ 7.14) and C-3′ ($\delta_C$ 149.4), H-5′ ($\delta_H$ 6.76) and C-3′ ($\delta_C$ 149.4) observed in an HMBC spectrum (ESM, Fig. S17). Thus, compound M3 was identified as 3′-methyl-5-CQA.

The material eluted as peak 2 ($t_R$ = 22.92–24.61 min, M4) (ESM, Fig. S16) showed an [M-H]$^-$ ion with *m/z* 367.1035, which in conjunction with the $^{13}$C NMR data corresponded to a molecular formula of $C_{17}H_{19}O_9$. The $^1$H and $^{13}$C NMR data of M4 in Table 2 showed M4 and M3 with similar structural characteristics. The HMBC data indicated that the location of the methoxyl group of M4 was different with that of M3. HMBC correlations were observed between the methoxy protons ($\delta_H$ 3.83) and C-4′ ($\delta_C$ 151.5) and between H-2′ ($\delta_H$ 7.03), H-5′ ($\delta_H$ 6.89), H-6′ ($\delta_H$ 7.01), and C-4′ ($\delta_C$ 151.5), placing the methoxy group at C-4′ (ESM, Fig. S17). Detailed analysis of the HSQC and HMBC data (ESM, Figs. S9–S12) allowed unambiguous assignments for all of the $^1$H and $^{13}$C NMR signals of M4. Accordingly, M4 was determined to be 4′-methyl-5-CQA.

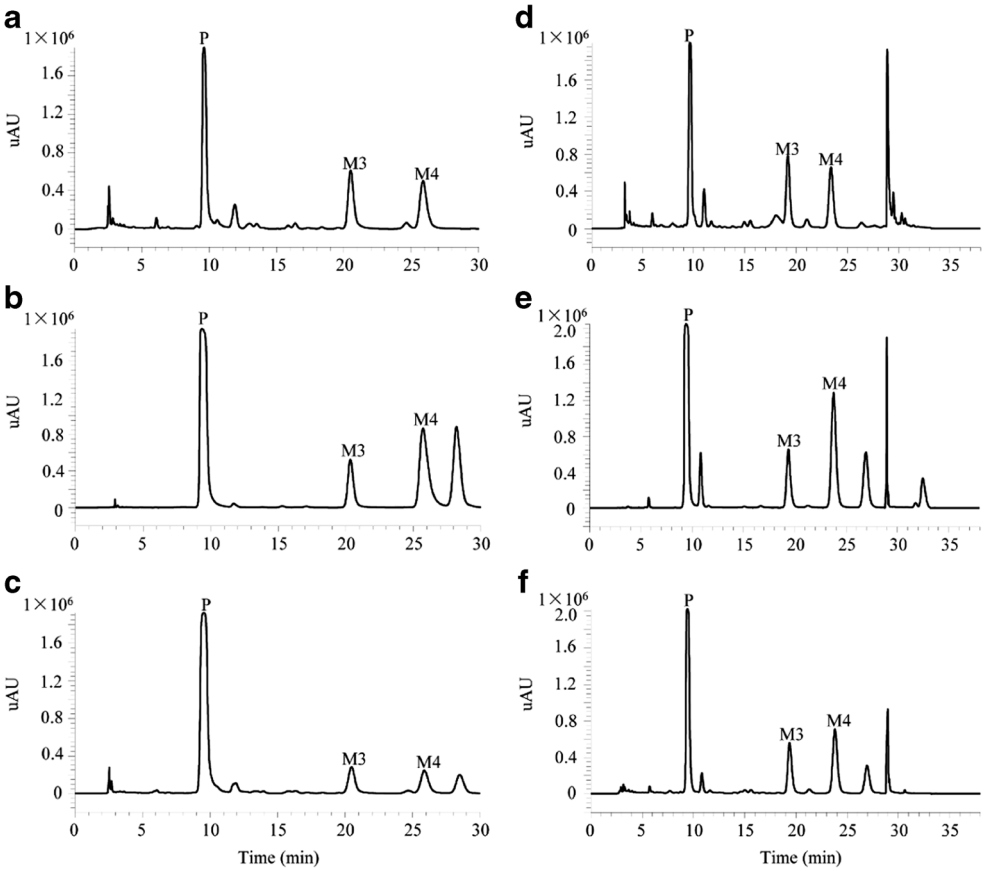


**Fig. 2** HPLC-UV chromatograms collected at 330 nm of M3 and M4 in human urine (**a**, **d**), synthetic system (**b**, **e**), and pooled samples (**c**, **f**). HPLC-UV chromatograms on the left side were analyzed by mode A. HPLC-UV chromatograms on the right side were analyzed by mode B

## Synthesis, isolation, and purification of M3 and M4

We used phase transfer catalyst tetra-n-butylammonium bromide to improve the methylation of 5-CQA. M3 and M4 were increased by 1.7 and 1.5 times, respectively. The relative content of the two methylated products in the mixture (in terms of the peak area) was 75% of that before the extraction with diethyl ether. Since dimethyl sulfate oxidizes the ODS filler, it is necessary to remove most of the remaining dimethyl sulfate to ensure further separation of the ODS column. The diethyl ether used here was aimed to remove excess dimethyl sulfate in the reaction system. However, the sulfuric acid produced by the decomposition of dimethyl sulfate was present in the aqueous phase, which could not be eliminated by diethyl ether extraction. Fortunately, sulfate ions in the aqueous phase could be removed by elution as they pass through the ODS column. Thus, after the reaction was completed, dimethyl sulfate was removed by extraction with diethyl ether, and the diethyl ether layer was discarded. The aqueous layer was then lyophilized and separated with the ODS column.

The synthetic sample was analyzed by HPLC (ESM, Fig. S18). The results showed that 5-CQA, two methylated products (M3 and M4) and other products were present in the reaction mixture.

The separation results of ODS column (ESM, Fig. S13) showed that M3 and M4 were enriched in the 40% methanol fraction (fraction E), and thus, this fraction is used for further purification of M3 and M4.

The fraction E which contained 5-CQA, M3, and M4 was purified by semipreparative HPLC. The results showed that 5-CQA, M3, and M4 were well separated (ESM, Fig. S14), and the collection time of M3 and M4 were 20.5–21.5 and 27.0–28.5 min, respectively. The eluates enriched in M3 and M4 were evaporated to appropriate volume and lyophilized to give about 8 mg pure product of M3 and 15 mg pure product of M4.

The 200 μL eluates of M3 and M4 were transferred to a centrifuge tube, respectively. The sample was centrifuged at 13000 rpm for 10 min and the supernatant was injected to HPLC system for analysis. The HPLC condition was the same as HPLC-UV analytical condition. As shown in Fig. 3, the purity of M3 and M4 were 96.1 and 99.3% (in terms of the peak area), respectively.

## Reverse molecular docking to predict activities of M3 and M4

PharmMapper is backed up by a large, in-house repertoire of pharmacophore database extracted from all the targets in TargetBank, DrugBank, BindingDB, and PDTD. Currently,

**Table 2** NMR spectroscopic data of 5-CQA, M3, and M4

| Position | 5-CQA | | M3 | | | M4 | | |
|---|---|---|---|---|---|---|---|---|
| | $\delta_C$, mult. | $\delta_H$ ($J$ in Hz) | $\delta_C$, mult. | $\delta_H$ ($J$ in Hz) | HMBC | $\delta_C$, mult. | $\delta_H$ ($J$ in Hz) | HMBC |
| 1 | 76.1, C | | 76.1, C | | | 76.1, C | | |
| 2 | 38.7, $CH_2$ | 2.02, m | 38.7, $CH_2$ | 2.10, m | 1, 3, 4 | 38.7, $CH_2$ | 2.10, m | 5 |
| | | 2.50, m | | 2.26, m | | | 2.25, m | 1, 4, 5 |
| 3 | 71.3, CH | 4.14, m | 71.2, CH | 4.12, m | 4 | 71.2, CH | 4.11, m | |
| 4 | 73.4, CH | 3.69, m | 73.4, CH | 3.68, m | 5 | 73.4, CH | 3.67, m | 5 |
| 5 | 72.0, CH | 5.30, m | 72.0, CH | 5.27, m | | 72, CH | 5.27, m | |
| 6 | 38.2, $CH_2$ | 2.05, m | 38.2, $CH_2$ | 2.04, m | 5 | 38.2, $CH_2$ | 2.03, m | 1, 3, 4 |
| | | 2.20, m | | 2.20, m | 1, 4, 5 | | 2.20, m | |
| 7 | 177.0, C | | 177.1, C | | | 177, C | | |
| 1′ | 127.8, C | | 127.8, C | | | 128.9, C | | |
| 2′ | 115.2, CH | 7.02, d (2.4) | 111.8, CH | 7.14, d (1.8) | 3′,4′,6′,7′ | 112.5, CH | 7.03, d (1.8) | 2′,3′,4′,6′,7′,8′ |
| 3′ | 146.8, C | | 149.4, C | | | 148, C | | |
| 4′ | 149.6, C | | 150.6, C | | | 151.5, C | | |
| 5′ | 116.5, CH | 6.75, d (8.4) | 116.5, CH | 6.76, d (7.8) | 1′,3′,4′ | 116.3, CH | 6.89, d (7.8) | 1′,3′,4′,6′,8′ |
| 6′ | 123.0, CH | 6.92, dd (2.4, 8.4) | 124.1, CH | 7.03, dd (1.8, 7.8) | 2′,4′,7′ | 122.8, CH | 7.01, dd (1.8, 7.8) | 2′,4′,6′,7′,8′ |
| 7′ | 147.1, CH | 7.53, d (16.2) | 147.0, CH | 7.57, d (16.2) | 1′,2′,6′,8′,9′ | 146.7, CH | 7.53, d (16.2) | 1′,5′,6′,8′,9′ |
| 8′ | 115.2, CH | 6.23, d (16.2) | 115.6, CH | 6.30, d (16.2) | 1′,9′ | 114.8, CH | 6.26, d (16.2) | 1′,9′ |
| 9′ | 168.6, C | | 168.7, C | | | 168.4, C | | |
| $OCH_3$-3′ | | | 56.5, $CH_3$ | 3.84, s | 3′ | | | |
| $OCH_3$-4′ | | | | | | 56.4, $CH_3$ | 3.83, s | 4′ |

[1] H NMR data ($\delta$) were measured in methanol-$d_4$ for 5-CQA, M3, and M4 at 600 MHz (cold probe). [13] C NMR data ($\delta$) were measured in methanol-$d_4$ for 5-CQA, M3, and M4 at 150 MHz (cold probe). The assignments were based on [1] H, [13] C, HSQC, and HMBC experiments

there are 7302 pharmacophore models in PharmTargetDB (Version 2010) and 2241 of them are annotated as the potential protein targets in Human (http://lilab.ecust.edu.cn/pharmmapper/).

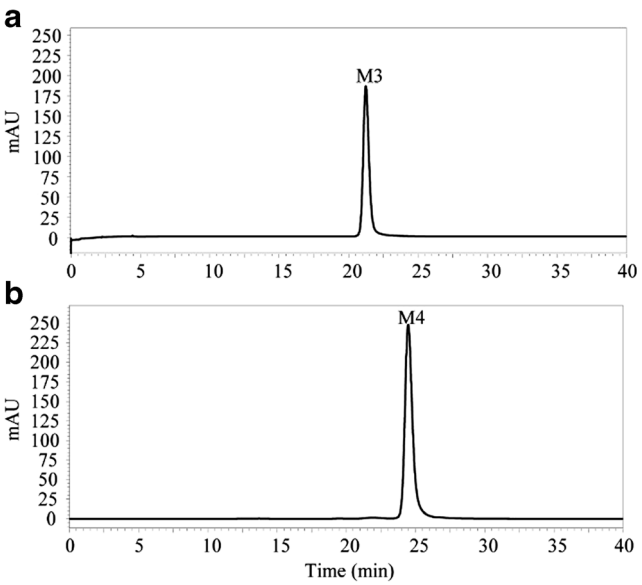


**Fig. 3** **a**, **b** HPLC-UV chromatograms of M3 and M4. The purity of M3 and M4 were 96.1 and 99.3% (in terms of the peak area)

In this study, firstly, the PharmTargetDB (Version 2010) was used to perform a reverse molecular analysis for the discovery of potential targets. The results showed that a total of 247 targets were obtained with a potential interaction with M3 and M4. Secondly, the 247 targets were labeled in eight malignant glioma-related pathways using KEGG (http://www.kegg.jp/). These typical pathways included the PI3K-Akt, mTOR, Ras, EGFR, MAPK, NF-kappa B, and Jak-STAT pathways and DNA replication [18–22], which based on the previous study of malignant glioma. It found to be that ten targets among 247 targets were labeled in eight malignant glioma-related pathways. As shown in Fig. 3, the network consists of two methylated metabolites (M3 and M4), ten targets, and eight malignant glioma-related pathways. As we can see, M3 hit seven targets among eight pathways, while M4 hit five targets among eight pathways. In addition, four targets were hit by both methylated metabolites. While DNA replication and PI3K-Akt and mTOR pathways were the top three pathways which contained the most targets (Fig. 4). The abovementioned results demonstrated the effects of M3 and M4 on targeting different receptors and pathways of malignant glioma.

The 5-CQA was also analyzed by the above method and 105 potential targets were obtained using the PharmTargetDB (Version 2010). Specifically, 5-CQA hit six targets among

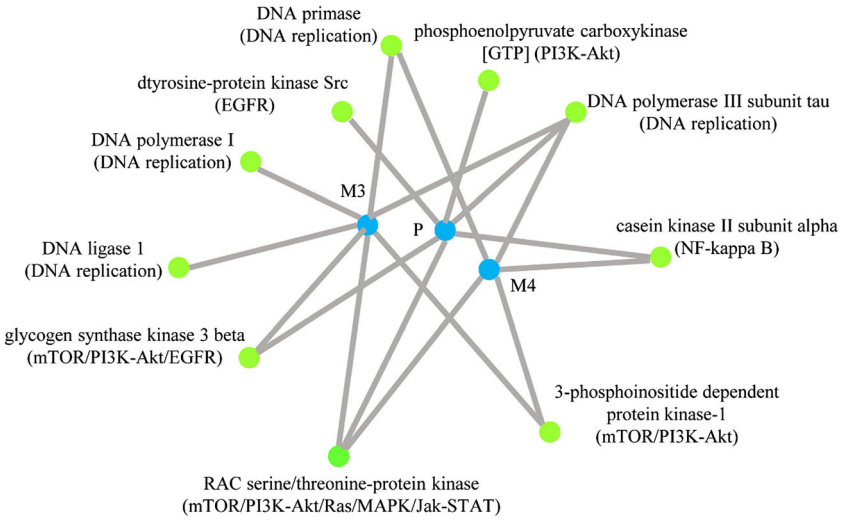


**Fig. 4** Network diagram of 5-CQA (P), methylated metabolites (M3 and M4), and their potential targets. Gray lines represent predicted interactions between P, M3, and M4 (circles filled in blue) and malignant glioma-related targets (circles filled in green) calculated by reverse docking

eight malignant glioma-related pathways and showed varieties of interactions with these targets (Fig. 4). Moreover, both RAC serine/threonine-protein kinase and DNA polymerase III subunit tau were hit by 5-CQA, M3, and M4. In addition, three targets were hit by both 5-CQA and M3, while three targets were hit by both 5-CQA and M4. It is speculated that M3 and M4 may have the anti-tumor activity like 5-CQA.

## Discussion

In this study, we constructed a work flow for the identification and preparation of trace amount of metabolites with similar structures and chromatographic behaviors after intramuscular administration of 5-CQA injection in humans. As shown in Fig. 5, a method involving HPLC-HRMS/MS$^n$ was developed for profiling 5-CQA and its metabolites in human urine and feces. In addition to 5-CQA, six metabolites were found in human urine. These metabolites can be classified into three main types, including isomerized 5-CQA (P1 and P2), hydrolyzed 5-CQA (M1 and M2) and methylated 5-CQA (M3 and M4). No metabolites were detected in the feces. Except for the parent drug, the methylated metabolites in urine samples showed the highest content (Fig. 1). However, the exact methylation site of M3 and M4 could not be confirmed with MS data merely. In order to annotate the structures of methylated metabolites, we tried to isolate M3 and M4 from human urine. Since the complex matrices and endogenous interference in human urine made it very difficult to get them with enough purity for NMR analysis, chemical synthesis of methylated 5-CQA was performed for structural annotation. The synthesized compounds were

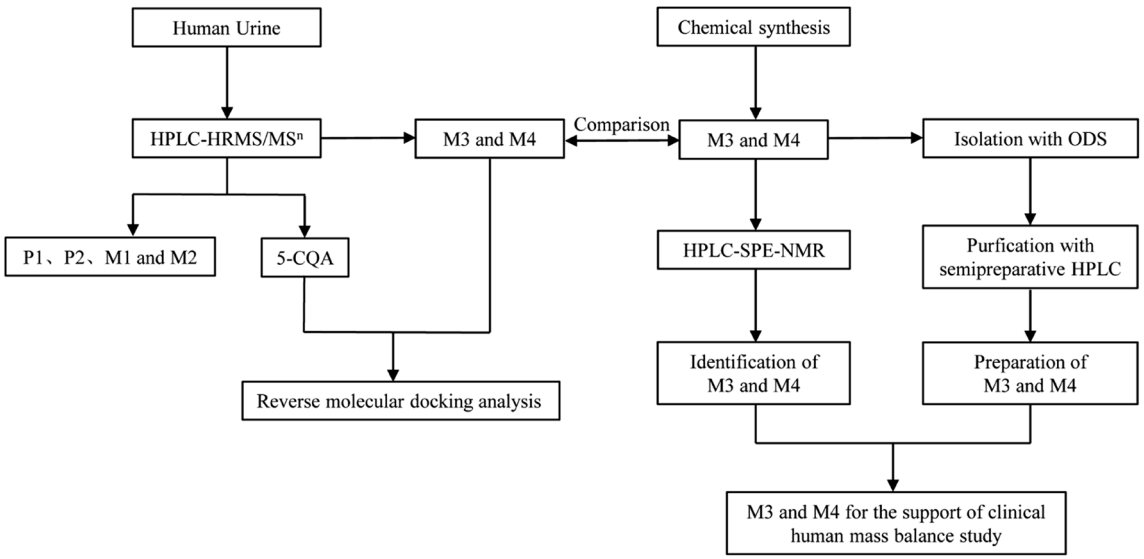


**Fig. 5** The work flow for identification and preparation of traces amount isomer with similar property in human urine after intramuscularly administered 5-CQA injection

confirmed as M3 and M4 identified in urine samples by comparing their retention time, HRMS and $MS^n$ data. In addition, since M3 and M4 were similar in HPLC behavior, the preparation of pure M3 and M4 for structure identification with NMR is a great task, and the synthesized mixture of M3 and M4 was directly analyzed by HPLC-SPE-NMR for rapid identification. At the same time, the synthetic mixture was separated with the ODS column following the isolation on semipreparative HPLC to harvest pure M3 and M4. Furthermore, the potential activity of M3 and M4 on malignant glioma was predicted using a reverse molecular docking analysis on eight malignant glioma-related pathways.

The Metwork 1.3 software was used to discover and identify metabolites of 5-CQA. The software contained a database which included the metabolism reactions in humans. In general, the structure of parent drug is imported into the software to search the database using HRMS data. The potential metabolites are discovered when the HRMS data is matched. Then the structures of potential metabolites are identified by examining retention time, HRMS and $MS^n$ data. The 5-CQA was reported to hydrolyze into quinic acid and caffeic acid [14]. In this study, quinic acid and reduced metabolite of caffeic acid were also detected as the metabolites of 5-CQA. The metabolic reaction of losing a quinic acid or caffeic acid, however, was not recorded in the Metwork database. To ensure the efficient discovery of metabolites, the structures of 5-CQA, quinic acid, and caffeic acid were all imported into the software for the discovery of the 5-CQA metabolites.

We used several HPLC conditions in this study. The HPLC condition in Fig. 1 was established for metabolic profile of human biosamples. The mode A and mode B in Fig. 2 were used to analysis human urine sample, chemical synthesis sample, and the pooled sample in order to confirm whether the methylated products M3 and M4 from chemical synthesis and human urine were the same compounds from RT data. According to the suitable confirmatory methods for identification of compounds (ESM, Table S4) in the EU Directive 2002-657-EC (http://eur-lex.europa.eu/eli/dec/2002/657/oj), we need to establish at least two different chromatographic systems to get different retention times of M3 and M4 in order to meet the limitation of LC-UV. So in this study, we used two different HPLC systems (mode A and mode B) to collect the spectra of M3 and M4 at 330 nm. As shown in revised Fig. 2, the retention times of M3 and M4 in the synthetic sample were equal to those in the urine sample as well as the pooled sample. So the methylated products M3 and M4 from chemical synthesis and human urine were identified as the same compounds.

The methylated metabolites M3 and M4 were synthesized using the raw materials of 5-CQA. The synthetic system was selected for the identification of M3 and M4 with a higher purity than urine matrix. To ensure the synthesized compounds being the right target, we compared the methylated metabolites from human urine with that of chemical synthesis. M3 in the synthetic sample and urine sample gave the same predominant ion at *m/z* 191 of $MS^2$ analysis and *m/z* 127 of $MS^3$ analysis. In addition, M3 had the same fragment ion at *m/z* 193, 173, 111, and 93 in both samples. Maximum permitted tolerances for relative ion intensities using a range of mass spectrometric techniques (ESM, Table S1) as well as the relationship between a range of classes of mass fragment and identification points earned (ESM, Table S2) were used to compared M3 in the synthetic sample with in urine sample according to EU Directive 2002-657-EC (http://eur-lex.europa.eu/eli/dec/2002/657/oj). It was found that M3 in two samples showed the same accurate mass to earn 2 identification points. Furthermore, the fragment ions at *m/z* 191 (relative intensity > 50%, relative ± 20%), 193 (relative intensity < 10%, relative ± 50%) and 173 (relative intensity< 10%, relative ± 50%) each earned 1.5 identification points. In total, M3 earned 6.5 identification points and had already achieved the criterion of 4 points to confirm M3 as the same compound in the synthetic sample and urine sample. M4 was compared as the same way. In summary, the use of synthetic samples instead of human urine samples for the identification and preparation of M3 and M4 was reasonable as well as reliable.

HPLC-SPE-NMR was used to unambiguously assign the methylation sites of M3 and M4 for the first time. The advantages of HPLC-SPE-NMR are as follows. Firstly, the combined benefits of analyte concentration and accumulation and use of deuterated solvents enable acquisition of high quality 2D NMR data from multiple peaks within a short time, including minor peaks present in very complex chromatograms. Secondly, access to less-sensitive 2D NMR experiments such as availability of $^{13}C$ chemical shifts (from HSQC and HMBC experiments) allows rigorous structure elucidation of rather complex natural products directly from extracts and mixtures [23, 24]. Finally, the large amounts of analytes available by multiple trapping allow the recording of NMR spectra with excellent signal-to-noise ratios without solvent peak suppression. The broad applicability of the technique to natural products has already been demonstrated, and the technique is envisaged to be an increasingly important analytical platform for natural products research. HPLC-SPE-NMR is expected to provide an increasing number of rigorously determined natural product structures directly from extracts and isolates, including compounds present in minor amounts [25]. Practical applications from both drug metabolite and drug impurity identification are presented [26]. Accordingly, M3 and M4 were determined by HPLC-SPE-NMR to be 3′-methyl-5-CQA and 4′-methyl- 5-CQA for the first time, respectively.

At the same time, the synthetic mixture was used to prepare the pure products of M3 and M4. The mixture was isolated with ODS column to yield fraction E which contained 5-CQA and two methylated products and was purified by semipreparative HPLC. The eluate, enriched in M3 and M4, was evaporated to appropriate volume and lyophilized to give about 8 mg pure product of M3 and 15 mg pure product of M4. The purity of M3 and M4 was 96.1 and 99.3% (in terms of the peak area), respectively.

To our best knowledge, it is the first time to obtain the standards of methylated 5-CQA (M3 and M4) for the support of clinical human mass balance study. Since the isolation and purification lasted for a long time, mixed reference standards from chemical synthesis may be used directly for clinical research when the ingredient ratio of M3 and M4 is marked.

The activity of M3 and M4 has not been studied previously. Reverse molecular docking analysis was conducted to predict the potential activity of M3 and M4 for malignant glioma on eight malignant glioma-related pathways. It found to be that 5-CQA hit six targets among eight pathways and showed varieties of reciprocity with these targets. M3 hit seven targets among eight pathways, while M4 hit five targets among eight pathways. Two targets were both hit by 5-CQA, M3, and M4. In addition, three targets were both hit by 5-CQA and M3, while three targets were both hit by 5-CQA and M4. Efforts were made to validate the prediction. Similar activities of 5-CQA have been reported in the literature, which showed potential interactions with the PI3K-Akt [27], mTOR [28], Ras [29], EGFR [30], MAPK [31–33], NF-kappa B [34], and Jak-STAT [35] pathways and DNA replication [36]. M3 and M4 had the similar interactions like 5-CQA among malignant glioma-related pathways, so they may play important roles in the treatment of malignant glioma. Further study will be needed to clarify the mechanisms of M3 and M4 in inhibiting the malignant glioma.

## Conclusion

In summary, HPLC-HRMS/MS$^n$ was used to profile the metabolites of 5-CQA injection in human urine and fecal samples. Six metabolites were identified in human urine, and 3′-methyl-5-CQA (M3) and 4′-methyl-5-CQA (M4) were the most abundant metabolites in humans except for 5-CQA. M3 and M4 were synthesized by 5-CQA methylation and followed by isolation and purification to harvest pure standards. The proposed structural identities of these two metabolites were supported by $^1$H, $^{13}$C, and 2D NMR data comparison with synthesized standards. According to reverse molecular docking results, M3 and M4 showed a various interactions with malignant glioma-related targets, indicating that M3 and M4 may have activities in the treatment of malignant glioma. To our best knowledge, this is the first time to clarify the structure of methylated metabolites of 5-CQA injection. These results contribute to our understanding of the metabolism of 5-CQA injection in humans and provide support for the clinical human mass balance study.

**Acknowledgements** The Ministry of Science and Technology of the People's Republic of China (2016ZX09101017) is acknowledged.

**Compliance with ethical standards** Informed consent was obtained from all individual participants who provided urine and feces samples. Ethics approval for this study has been obtained from the Ethics Committee, Beijing Shijitan Hospital, China.

**Conflict of interest** The authors declare that they have no conflicts of interest.

## References

1. Xie C, et al. Identification of the ortho-benzoquinone intermediate of 5-O-caffeoylquinic acid in vitro and in vivo: comparison of bioactivation under normal and pathological situations. Drug Metab Dispos. 2012;40(8):1628–40.
2. Upadhyay R, Mohan Rao LJ. An outlook on chlorogenic acids-occurrence, chemistry, technology, and biological activities. Crit Rev Food Sci Nutr. 2013;53(9):968–84.
3. Clifford MN. Chlorogenic acids and other cinnamates-nature, occurrence, dietary burden, absorption and metabolism. J Sci Food Agric. 2000;80:1033–43.
4. dos Santos MD, et al. Evaluation of the anti-inflammatory, analgesic and antipyretic activities of the natural polyphenol chlorogenic acid. Biol Pharm Bull. 2006;29(11):2236–40.
5. Kono Y, et al. Antioxidant activity of polyphenolics in diets. Rate constants of reactions of chlorogenic acid and caffeic acid with reactive species of oxygen and nitrogen. Biochim Biophys Acta. 1997;1335(3):335–42.
6. Kasai H, et al. Action of chlorogenic acid in vegetables and fruits as an inhibitor of 8-hydroxydeoxyguanosine formation in vitro and in a rat carcinogenesis model. Food Chem Toxicol. 2000;38(5):467–71.
7. Liang N and Kitts DD. Role of chlorogenic acids in controlling oxidative and inflammatory stress conditions. Nutrients. 2015. 8(1). https://doi.org/10.3390/nu8010016.
8. Bandyopadhyay G, et al. Chlorogenic acid inhibits Bcr-Abl tyrosine kinase and triggers p38 mitogen-activated protein kinase-dependent apoptosis in chronic myelogenous leukemic cells. Blood. 2004;104(8):2514–22.
9. Jaroszewski JW. Hyphenated NMR methods in natural products research, part 2: HPLC-SPE-NMR and other new trends in NMR hyphenation. Planta Med. 2005;71(9):795–802.
10. Park JJ, et al. Chlorogenic acid inhibits hypoxia-induced angiogenesis via down-regulation of the HIF-1alpha/AKT pathway. Cell Oncol. 2015;38(2):111–8.
11. Zhukova I, et al. Long-term experience with lovastatin treatment in patients with coronary heart disease and hyperlipoproteinaemia type II. Eur Heart J. 1992;13(Suppl B):7–10.
12. Cope TM, Hunter JM. Selecting neuromuscular-blocking drugs for elderly patients. Drugs Aging. 2003;20(2):125–40.
13. Muth-Selbach U, et al. Antinociceptive effects of systemic lidocaine: involvement of the spinal glycinergic system. Eur J Pharmacol. 2009;613(1–3):68–73.
14. Azuma K, et al. Absorption of chlorogenic acid and caffeic acid in rats after oral administration. J Agric Food Chem. 2000;48(11):5496–500.

15. Booth AN, et al. Urinary metabolites of caffeic and chlorogenic acids. J Biol Chem. 1957;229(1):51–9.
16. Xie C, et al. Metabolites of injected chlorogenic acid in rats. Yao Xue Xue Bao. 2011;46(1):88–95.
17. Wang C, et al. Pharmacokinetics of 21 active components in focal cerebral ischemic rats after oral administration of the active fraction of Xiao-Xu-Ming decoction. J Pharm Biomed Anal. 2016;122:110–7.
18. Huang TT, et al. Targeted therapy for malignant glioma patients: lessons learned and the road ahead. Neurotherapeutics. 2009;6(3): 500–12.
19. Mellinghoff IK, et al. Signal transduction inhibitors and antiangiogenic therapies for malignant glioma. Glia. 2011;59(8): 1205–12.
20. Guo G, et al. Oleanolic acid suppresses migration and invasion of malignant glioma cells by inactivating MAPK/ERK signaling pathway. PLoS One. 2013;8(8):e72079.
21. Chen X, et al. The regulator of calcineurin 1 (RCAN1) inhibits nuclear factor kappaB signaling pathway and suppresses human malignant glioma cells growth. Oncotarget. 2017;8(7):12003–12.
22. Chang JH, et al. MicroRNA-203 modulates the radiation sensitivity of human malignant glioma cells. Int J Radiat Oncol Biol Phys. 2016;94(2):412–20.
23. Clarkson C, et al. Hyphenation of solid-phase extraction and nuclear magnetic resonance: application of HPLC-DAD-SPE-NMR to identification of constituents of *Kanahia laniflora*. Anal Chem. 2005;77(11):3547–53.
24. Pukalskas A, et al. Development of a triple hyphenated HPLC-radical scavenging detection-DAD-SPE-NMR system for the rapid identification of antioxidants in complex plant extracts. J Chromatogr A. 2005;1074(1–2):81–8.
25. Jin UH, et al. A phenolic compound, 5-caffeoylquinic acid (chlorogenic acid), is a new type and strong matrix metalloproteinase-9 inhibitor: isolation and identification from methanol extract of *Euonymus alatus*. Life Sci. 2005;77(22): 2760–9.
26. Sandvoss M, et al. HPLC-SPE-NMR in pharmaceutical development: capabilities and applications. Magn Reson Chem. 2005;43(9):762–70.
27. Xue N, et al. Chlorogenic acid inhibits glioblastoma growth through repolarizating macrophage from M2 to M1 phenotype. Sci Rep. 2017;7:39011.
28. Han D, et al. Cytoprotective effect of chlorogenic acid against hydrogen peroxide-induced oxidative stress in MC3T3-E1 cells through PI3K/Akt-mediated Nrf2/HO-1 signaling pathway. Oncotarget. 2017;8(9):14680–92.
29. Banerjee N, et al. Plum polyphenols inhibit colorectal aberrant crypt foci formation in rats: potential role of the miR-143/protein kinase B/mammalian target of rapamycin axis. Nutr Res. 2016;36(10): 1105–13.
30. Hou Y, et al. Qingfei Xiaoyan Wan, a traditional Chinese medicine formula, ameliorates Pseudomonas aeruginosa-induced acute lung inflammation by regulation of PI3K/AKT and Ras/MAPK pathways. Acta Pharm Sin B. 2016;6(3):212–21.
31. Lee YJ, et al. Upregulation of caveolin-1 by mulberry leaf extract and its major components, chlorogenic acid derivatives, attenuates alcoholic steatohepatitis via inhibition of oxidative stress. Food Funct. 2017;8(1):397–405.
32. Tsai CM, et al. Assessment of the anti-invasion potential and mechanism of select cinnamic acid derivatives on human lung adenocarcinoma cells. Mol Pharm. 2013;10(5):1890–900.
33. Lee CH, et al. Chlorogenic acid attenuates high mobility group box 1 (HMGB1) and enhances host defense mechanisms in murine sepsis. Mol Med. 2013;22(18):1437–48.
34. Ji L, et al. Chlorogenic acid, a dietary polyphenol, protects acetaminophen-induced liver injury and its mechanism. J Nutr Biochem. 2013;24(11):1911–9.
35. Wu XL, et al. Anti-inflammatory effect of supercritical-carbon dioxide fluid extract from flowers and buds of *Chrysanthemum indicum* Linnén. Evid Based Complement Alternat Med. 2013;2013:413237.
36. Zhao Y, et al. UFLC/MS-IT-TOF guided isolation of anti-HBV active chlorogenic acid analogues from *Artemisia capillaris* as a traditional Chinese herb for the treatment of hepatitis. J Ethnopharmacol. 2014;28(156):147–54.